ARTICLE
Journal of Cellular Biochemistry 116:1213–1221 (2015)

Journal of Cellular Biochemistry

miR-155 Regulates Glioma Cells Invasion and Chemosensitivity by p38 Isforms In Vitro

Qiang Liu,[1,2] Ran Zou,[1] Rouxi Zhou,[3] Chaofan Gong,[3] Zhifei Wang,[2] Tao Cai,[2] Chaochao Tan,[2] and Jiasheng Fang[1*]

[1]*Department of Neurosurgery, Xiangya Hospital, Central South University, Changsha, Hunan, PR China*
[2]*Department of Neurosurgery, The Third Xiangya Hospital, Central South University, Changsha, Hunan, PR China*
[3]*Xiangya Medical School, Central South University, Changsha, Hunan, PR China*

ABSTRACT

The critical role of microRNAs in cancer development has been extensively described. miRNAs are both specific markers and putative therapy targets. miR-155 has been identified to be an oncomiRNA and is highly expressed in several solid cancers, including glioblastoma. In this study, we found that miR-155 is a good potential therapy target. Knockdown of miR-155 sensitizes glioma cells to the chemotherapy of temozolomide (TMZ) by targeting the p38 isoforms mitogen-activated protein kinase 13 [MAPK13, also known as p38 MAPKδ or stress-activated protein kinase 4 (SAPK4)] and MAPK14 (also known as p38 MAPKα). As tumor suppressor genes, MAPK13 and MAPK14 play important roles in lowering the accumulation of reactive oxygen species (ROS), inducing cell apoptosis, and slowing the progression of cancer. Knockdown of miR-155 enhanced the anticancer effect of TMZ on glioma by targeting the MAPK13 and MAPK14-mediated oxidative stress and apoptosis, but did not affect the secretion of MMP2 and MMP9. J. Cell. Biochem. 116: 1213–1221, 2015.

KEY WORDS: microRNA; MAPK; TEMOZOLOMIDE; REACTIVE OXYGEN SPECIES; CHEMOSENSITIVITY; GLIOBLASTOMA

MicroRNAs (miRNAs) play a critical role in tumorigenesis and are involved in the initiation and progression of cancer through post-transcriptional modifications. Additionally, miRNAs are considered to be potential biomarkers for cancer diagnosis and treatment monitoring [Lee et al., 2012; Liu et al., 2012; Sandhu et al., 2012]. miR-155 was first shown to be expressed at high levels in diffuse large B cell lymphomas (DLBCLs) that have an activated B cell phenotype [Eis et al., 2005]. Multiple studies have established that miR-155 is one of the most overexpressed miRNAs in several solid cancers, such as breast cancer [Volinia et al., 2006; Iorio et al., 2005; Mattiske et al., 2012], lung cancer [Volinia et al., 2006; Yang et al., 2013], stomach carcinoma [Volinia et al., 2006], prostate cancer [Volinia et al., 2006; Yang et al., 2013], colorectal carcinoma [Yang et al., 2013], and pancreatic carcinomas [Volinia et al., 2006; Yang et al., 2013]. The high expression of miR-155 is also a potential diagnosis marker for solid cancers. For example, a high expression pattern of miR-155 could be used as an adjunctive diagnostic tool or a clinically relevant biomarker for pulmonary NE tumors [Lee et al., 2012]. In addition, the levels of circulating miR-155 in the plasma may serve as a reliable, novel, and noninvasive biomarker for early diagnosis and detection of esophageal cancer [Liu et al., 2012].

Gliomas are the most common malignant tumors in the adult central nervous system and account for 50 to 60% of primary brain tumors. The characteristic of glioma is extensive invasion throughout the brain and a poor prognosis [Ohgaki and Kleihues, 2005]. Studies have shown that miR-155 is high expressed in the primary and secondary glioblastoma tissues [D′Urso et al., 2012]. Knockdown of miR-155 inhibited the cell proliferation and GABA-A receptor regulating signaling pathway in glioblastoma primary culture cells [Poltronieri et al., 2013]. Inhibiting the expression of miR-155 can enhance the chemosensitivity of glioblastoma cells to taxol by targeting EAG1 expression [Meng et al., 2012].

miRNAs have emerged as key regulators of gene expression; they can repress gene expression through sequence-specific base pairing with a binding site in the 3′UTRs, 5′UTRs, or CDS of target transcripts [Bartel, 2004; Tay et al., 2008]. Up to now, there have 147 target genes of miR-155 validated. They are mainly involved in many biological behaviors, such as proliferation, differentiation, apopto-

Conflict of Interest: none.
*Correspondence to: Jiasheng Fang, Department of Neurosurgery, Xiangya Hospital, Central South University, Changsha, Hunan, 410008, PR. China. E-mail: 16630735@qq.com
Manuscript Received: 13 November 2013; Manuscript Accepted: 18 December 2014
Accepted manuscript online in Wiley Online Library (wileyonlinelibrary.com): 23 December 2014
DOI 10.1002/jcb.25073 • © 2014 Wiley Periodicals, Inc.

sis, angiogenesis and epithelial-msenchymal transition, and provide the prospects for the application potential of miR-155 [Volinia et al., 2006].

In this study, we detected the expression of human miR-155 in various differential grade glioma tissues and cell lines and designated this miRNA as a marker for the prognosis of glioma. Importantly, knockdown of miR-155 inhibits cell growth and invasion by targeting the p38 isoform that mediates ROS activity and apoptosis.

MATERIALS AND METHODS

CELL CULTURE

Six human glioma-derived cell lines, U251, U87, A172, SF767, SF126, and SHG-44 were obtained from the Cell Center of the Peking Union Medical College in China. U251, U87, and A172 cells were maintained in Dulbecco′s Modified Eagle′s Medium (DMEM) with 10% fetal calf serum (FCS) and standard antibiotics. SF767, SF126, and HG-44 cells were maintained in modified Eagle′s medium (MEM) with 10% fetal calf serum (FCS) and standard antibiotics. All cells were maintained at 37°C under an atmosphere of 5% CO_2 and 95% air.

PATIENT SAMPLES

All human primary brain tumor samples were obtained from randomly selected cancer patients at the Xiangya Hospital, Hunan, China, and all of the diagnoses were pathologically confirmed. Written informed consent was obtained from each patient who participated in the study before surgery, and all of the protocols were reviewed by the Joint Ethics Committee of the Central South University Health Authority and performed in accordance with national guidelines.

IN SITU HYBRIDIZATION ANALYSIS

The miR-155 miRCURYTM LNA custom detection probe (Exiqon, Vedbaek, Denmark) was used for the in situ hybridization (ISH). Hybridization, washing, and scanning were performed according to the manuals and protocols that were provided by the Exiqon life science department, and staining assessments were performed by two independent pathologists. Staining intensity was scored as 0 (negative), 1 + (weak), 2 + (medium), or 3 + (strong). Low expression was defined as an intensity of 0, 1, 2, or 3 with $<10\%$ stained cells or by an intensity of 0 or 1 with $<50\%$ stained cells. High expression was defined as an intensity of 2 or 3 with $>10\%$ stained cells or by an intensity of 1, 2, or 3 with $>50\%$ stained cells [Tang et al., 2013].

MTT ASSAY

Synthesized RNA duplexes of negative control, miR-155 mimics, and miR-155 inhibitors were obtained from GeneChem (GeneChem, Shanghai, China). After transient transfection of miRNA mimics or inhibitors, the cells were seeded into 96-well plates at 1500 cells/well, and the MTT assays (Sigma-Aldrich, St. Louis, MO, USA) were performed daily for 48 h. In this assay, the medium was replaced with fresh medium containing 0.5 mg/ml MTT for 4 h and then carefully removed. Subsequently, 150 μl of dimethyl sulfoxide (DMSO) was added to each well and mixed for 10 min. The optical density at 490 nm was determined using an enzyme linked immunosorbent assay (ELISA) reader.

INVASION AND MIGRATION ASSAYS

Invasion assays were performed using Transwell® plates (Corning, Corning, NY). Matrigel (Becton Dickinson, (Bedford, MA)) was diluted in cold serum-free medium, and 25 μg of the preparation was added to the top side of porous filters (pore size, 8 μm) and allowed to gel at 37°C overnight. After the coated filters were rehydrated with 100 μl medium, 1×10^5 cells in 200 μl of serum-free medium supplemented with 0.2% bovine serum albumin were seeded into the upper part of each chamber, and the lower compartments were filled with 500 μl of culture medium. Following incubation for 24 h in a humidified incubator at 37°C with 5% CO_2, cells that had not invaded on the upper surface of the filter were wiped out with a cotton swab, and the cells that had invaded on the lower surface of the filter were fixed and stained with hematoxylin. Invasiveness was determined by counting cells in four microscopic fields per well, and the extent of invasion was expressed as an average number of cells per microscopic field. The results are expressed as the mean ± SD.

Cell migration was evaluated by using the scratch wound assay; cells with or without treatment were cultured to 90% confluence and washed with serum-free medium. Then, the respective cell monolayers were disrupted by scratching with a 10-μL plastic pipette tip, and the wounded areas were photographed using an inverted microscope. The furthest distance that cells migrated from the wound edge was measured and the extent of migration was expressed as an average value of five independent microscope fields. The experiments were repeated three times and the results are expressed as the mean ± SD.

REAL-TIME QUANTITATIVE PCR ANALYSIS

Total RNA was extracted from the cells with TRIZOL reagent (Invitrogen, Carlsbad, CA), and human β-*actin* was amplified in parallel as an internal control. RT and PCR reactions were performed using a qSYBR green-containing PCR kit (Invitrogen, Carlsbad, CA), and human β-*actin* or U6 snRNA was used as an endogenous control for mRNA or miRNA detection, respectively. Expression of each gene was quantified by measuring the Ct values and normalized using the $2^{-\Delta\Delta dt}$ method relative to U6-snRNA or β-*actin*.

LUCIFERASE ASSAY

The MAPK13 and MAPK14 3′UTRs were cloned into the Sac1 and Mlu1 sites of the pMIR-REPORT luciferase vector (Ambion, Austin, TX) using a PCR-generated fragment that was designed using the Targetscan 6.1 software. Luc-mut vectors with the first five nucleotides, which are complementary to miR-155 seed regions, were mutated by site-directed mutagenesis (Stratagene, CA) and used as controls. The MAPK13 3′UTR primers were forward 5′-CCTACAAACGACACCCTG-3′ and reverse 5′-ATCCCTTCTGATCT-CAACAA -3′. The MAPK14 3′UTR primers were forward 5′-GCTGGGAGGGAAGGTGAA-3′ and reverse 5′-TTGATTTGGCGGTG-GATG-3′. The Luc-wt, Luc-mut, and Luc-ctrl plasmids were co-transfected with miR-155 mimics into HEK293 cells, and the pMIR-REPORT β-galactosidase control vector was transfected as a

control. Luciferase activity was measured in cell lysates 48 h after transfection using the Dual-Light® Luminescent Reporter Gene Assay kit (Applied Biosystems, Carlsbad, CA). The pMIR-REPORT™-β-gal control vector was co-transfected as an internal control to correct for differences in the transfection and harvest efficiencies.

MAPK13 AND MAPK14 SILENCING BY siRNAs

The sense sequences of the siRNA oligonucleotides that targeted *MAPK13* and *MAPK14* were the following: MAPK13 siRNA, sense strand siRNA 5′-GCACAUCUACAAGGAGAUUTT-3′ and antisense strand siRNA 5′-AAUCUCCUUGUAGAUGUGCTG-3′; MAPK14 siRNA, sense strand siRNA 5′-CUGCGGUUACUUAAACAUATT-3′ and antisense strand siRNA 5′-UAUGUUUAAGUAACCGCAGTT -3′ (Sangon, Shanghai). A scrambled siRNA was used as a negative control. The cells were plated in culture dishes or in 6-well plates for 24 h and transfected with siRNA using Lipofectamine 2000 (Invitrogen) for 48 h. The cells were then subjected to further assays or to RNA and protein extraction.

FLOW CYTOMETRY ASSAY

Annexin V/propidium iodide staining and flow cytometry were performed using the Annexin V-fluorescein isothiocynate Apoptosis Detection Kit (KeyGen, Nanjing, China) according to the manufacturer's guidelines. Briefly, 5×10^5 cells were washed in ice-cold PBS, resuspended in 50 μl of binding buffer and incubated with 2 μl of propidium iodide and 2 μl of Annexin V-fluorescein isothiocynate for 15 min in the dark at room temperature, washed and resuspended in 500 μl PBS. Flow cytometric analysis was performed immediately using a FACSCalibur (Becton Dickinson, San Jose, CA).

DETECTION OF MMP2 AND MMP9 BY ELISA

Glioma cells in subconfluent culture condition (~80–90% confluent) were washed and treated with or without miR-155, MAPK13 siRNA, or MAPK14 siRNA for 24 h. The conditioned serum-free medium was collected, centrifuged, and frozen at − 70°C until assayed. The protein concentrations of total MMP2 and MMP9 (pro- and active MMP9) in the culture supernatants were measured using ELISA kits (Boster Biotech, China) according to the manufacturer's instructions. The experiments were performed in triplicate and repeated once. The results are expressed as the mean ± SE.

WESTERN BLOT

Western blots were performed as previously described [Tang et al., 2013]. Anti-MAPK13 and MAPK14 antibodies were obtained from Cell Signaling Technology (Danvers, MA, USA) and β-actin antibodies were obtained from Santa Cruz Biotechnology (Santa Cruz, CA, USA).

APOPTOSIS DETECTION ASSAY

To morphologically detect apoptosis, treated or untreated cells were cultured for 48 h, fixed with 4% paraformaldehyde, and stained with Hoechst 33258 (0.5 μg/ml) for 15 min.

INTRACELLULAR REACTIVE OXYGEN SPECIES MEASUREMENT

The production of reactive oxygen species (ROS) was measured using the ROS-sensitive dye carboxy- 2, 7-dichlorodihydro-fluorescein diacetate (H2DCFDA, Invitrogen) as an indicator. Briefly, glioma cells were homogenized in assay buffer, and the homogenates were incubated with H2DCFDA at 37 °C for 3 h. The fluorescent product that was formed was quantified using a spectrofluorometer that was set at 485/525 nm (Beckman, USA), and changes in fluorescence were expressed in arbitrary units. Nacetylcysteine (NAC) was purchased from Sigma (USA).

STATISTICAL ANALYSIS

Differences between the variables of groups were tested using Student's *t* test or a one-way ANOVA using the SPSS 11.0 program. A *P*-value of <0.05 was considered statistically significant.

RESULTS

DIFFERENTIAL EXPRESSION OF miR-155 BETWEEN NORMAL CEREBRUM AND GLIOMA TISSUES

The level of expression of miR-155 was investigated in 24 normal brain tissues and 66 glioma tissues by in situ hybridization analysis (Fig 1A). The staining of miR-155 was strong and was detected in the cytoplasm of cells in 93.93% (62/66) glioma tissue samples. In contrast, miR-155 staining was undetectable or low in most of the normal cerebrums with positive staining in only 8.3% (3/24) of the samples. More importantly, we also found that the staining of miR-155 in astrocytomas was gradually enhanced with the increase in WHO grade from II to III and was accompanied by the proliferation of blood vessels in grade IV astrocytomas (Fig. 1A). The upregulated expression of miR-155 in grade IV astrocytomas (glioblastoma) was consistent with the results reported by D'Urso (2012). To confirm these findings, RNAs were extracted from 10 normal cerebrum samples and 42 astrocytoma samples and analyzed by real-time PCR (Fig. 1B). Consistent with the in situ hybridization data, the results demonstrated that in astrocytoma WHO grade II, III and IV, the expression of miR-155 was higher than that in the normal cerebrum samples and gradually enhanced with the increase in WHO grade from II to IV (Fig. 1B).

miR-155 REGULATES CELL INVASIVE GROWTH IN GLIOMA TISSUES

We detected the expression of miR-155 in six glioma cell lines by real-time PCR assay. We found that miR-155 was expressed the highest in U87 cells, whereas, the lowest expression was in SFF767 cells (Fig. 2A). Therefore, we chose to use the U87 and SF767 cells to perform our research. We over-expressed miR-155 in SF767 cells through transfection of miR-155 mimics, and we interfered with the expression of miR-155 in U87 cells through transfection of a miR-155 inhibitor. As expected, the miR-155 mimics promoted the expression of miR-155 in SF767 cells, and the miR-155 inhibitor significantly suppressed the expression of miR-155 in U87 cells at 96 h post-transfection (Fig. 2B). Next, we investigated cell growth in SF767 cells expressing the miR-155 mimics and found that cell growth was promoted in these cells. We also noted a decrease in cell viability and proliferation for U87 cells transfected with the miR-155 inhibitor at 96 h (Fig 2C).

To observe the effect of miR-155 on the invasion potential of SF767 and U87 cells, we performed a Matrigel matrix invasion assay

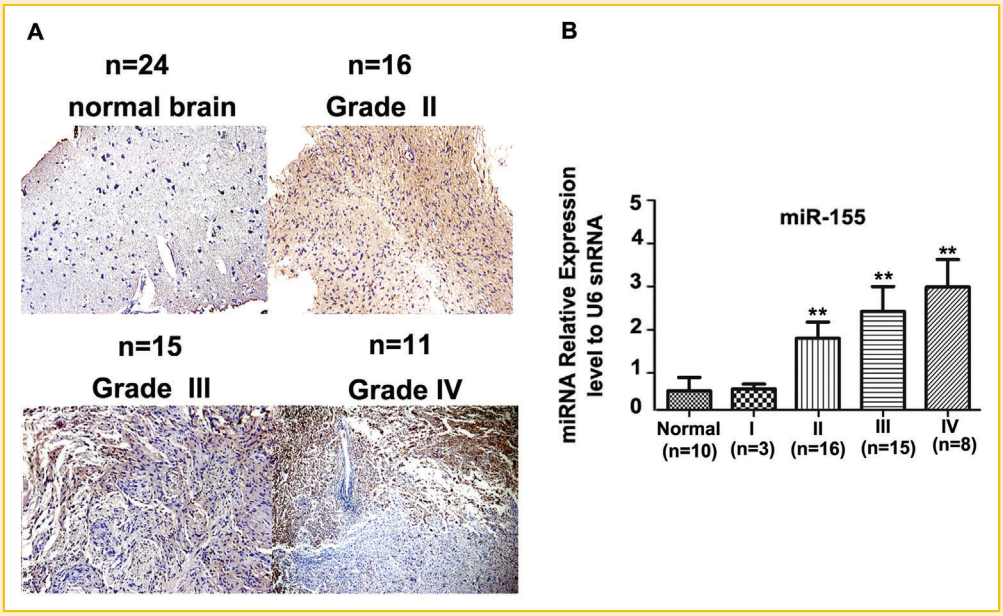

Fig. 1. Up-regulation of miR-155 in different WHO grade astrocytomas. A. ISH analysis of miR-155 in paraffin-embedded tissue sections from gliomas and normal brain tissues. The photomicrograph shows: normal brain tissue showing no or lowed expression of miR-155; grade II- IV showing immunopositivity and the staining of miR-155 in astrocytomas that is gradually enhanced with increase in WHO grade from II to III (original magnification100 ×). B. Histogram showing the mean expression +/− 95% confidence intervals for normal cerebrums and different WHO grade astrocytomas. ***P*-value <0.01 versus normal.

(Fig. 2D). When SF767 cells were treated with the miR-155 mimics, the invasion ability of cells increased compared to the invasion of cells treated with the negative control ($P < 0.05$). In contrast, when U87 cells were treated with the miR-155 inhibitor, invasion of U87 cells was inhibited compared with the invasion ability of cells treated with the negative control ($P < 0.01$).

To further investigate the cell migration ability at shorter incubation times, wound healing assay was used to detect cell migration ability after cells were cultured for 24 h and 48 h. The miR-155 mimics significantly promoted SF767 cell migration compared with the negative control transfected cells ($P < 0.01$), whereas, knockdown of miR-155 inhibited migration of U87 cells ($P < 0.05$) (Fig. 2E).

p38 ISOFORMS MAPK13 AND MAPK14 ARE THE TARGET GENES OF miR-155

To further understand the mechanism of miR-155-regulated glioma cell growth and invasion, TARGETSCAN 6.1 software was utilized to predict the miR-155 target genes. We found that MAPK13 and MAPK14 are potential target genes of miR-155. MAPK13 and MAPK14 are the isoforms of p38 and are also known as p38 delta and p38 alpha, respectively [Tan et al., 2010; Paillas et al., 2012]. p38 is a key member of the mitogen activated protein kinase (MAPK) family. The MAPK family pathway is implicated in diverse cellular processes, and its evolution is conserved throughout the eukaryotic kingdom [Li et al., 2011]. Our data verified that miR-155 could interact with the 3′UTR of MAPK13 and MAPK14 in the luciferase assay (Fig. 3A). The miR-155 mimics inhibited the expression of MAPK13 and MAPK14 at the mRNA (Fig. 3B) and protein level (Fig. 3C). To elaborate whether miR-155 affects the invasion of glioma cells by targeting MAPK13 and MAPK14, MAPK13 siRNA, or MAPK14 siRNA were transfected into SF767 cells, the matrigel matrix invasion assay was detected. As shown in Fig. 3D, MAPK13 siRNA, or MAPK14 siRNA promoted the cell invasion of SF767 cells.

miR-155 REGULATES THE SECRETION OF MMP2 AND MMP9 BY TARGETING THE p38 ISOFORMS MAPK13 OR MAPK14

Matrix metalloproteinases (MMPs) contribute to cancer through their involvement in cancer invasion and metastasis [Slattery et al., 2013]. To further determine whether miR-155 affects the secretion of MMP2 and MMP9 by targeting MAPK13 and MAPK14, miR-155 mimics, MAPK13 siRNA, or MAPK14 siRNA were transfected into SF767 cells, and the secretion of MMP2 and MMP9 was detected by ELISA. Compared with the negative control, miR-155 mimics increased the secretion of MMP2 and MMP9 (Fig. 4A). In contrast, MAPK13 siRNA or MAPK14 siRNA significantly decreased MAPK13 or MAPK14 expression, respectively, and increased the secretion of MMP2 and MMP9 (Fig. 4B). These results suggest that miR-155 increased the secretion of MMP2 and MMP9 by targeting MAPK13 and MAPK14 expression.

Knockdown of miR-155 sensitizes human primary glioblastoma cells to the ROS-induced apoptosis by the chemotherapeutic drug temozolomide

To investigate whether knockdown of miR-155 affects the inhibition of temozolomide (TMZ) on glioma cells, U87 cells were used to evaluate the anti-tumor effects of the designed treatments (i.e., miR-155 inhibitor for 6 h, followed by a subsequent TMZ treatment) in vitro. When we knocked down miR-155 for 6 h followed by a subsequent TMZ treatment, the MTT assay indicated that the combined knockdown of miR-155 and TMZ resulted in a

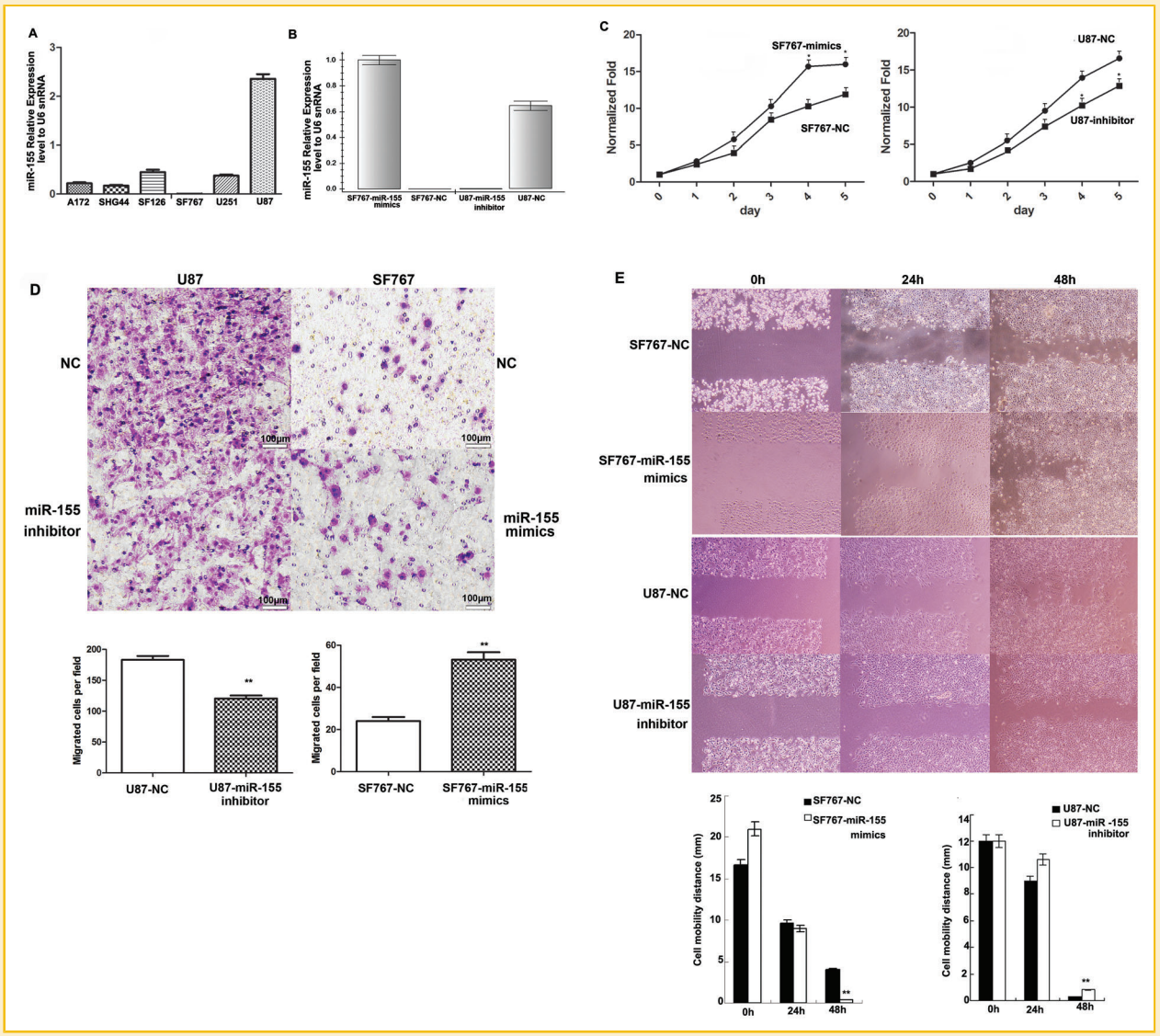

Fig. 2. miR-155 regulates the growth and invasion of glioma cells. A: The expression of miR-155 in the six glioma cell lines. The expression of miR-155 is the highest in the U87 cells, and it is the lowest in the SFF767 cells. B: Transfection efficiency of miR-155 mimics in SF767 cells or miR-155 inhibitor in U87 cells. C: The MTT assay was used to detect the effect of miR-155 on glioma cells. miR-155 mimics promoted the proliferation of SF767 cells, and miR-155 inhibitor suppressed the proliferation of U87 cells. The experiments were repeated three times. **P*-value <0.05. ** *P*-value <0.01 versus NC. D: The Matrigel matrix invasion assay was used to detect the effect of miR-155 on glioma cells. miR-155 mimics promoted the invasion of SF767 cells, and the miR-155 inhibitor suppressed the invasion of U87 cells. The histogram represents the mean of invasive cells which was determined by counting cells in four microscopic fields per well. The experiments were repeated three times. * *P*-value <0.05 versus NC. ** *P*-value <0.01 versus NC. E: The wound healing assay was used to detect the effect of miR-155 on glioma cells. miR-155 mimics promoted the migration of SF767 cells, and the miR-155 inhibitor suppressed the migration of U87 cells. The histogram represents the extent of migration which is expressed as an average value of five independent microscope fields. The experiments were repeated three times. * *P*-value <0.05 versu. NC. ** *P*-value <0.01 versus NC.

distinct decrease in U87 cell proliferation compared with miR-155 knockdown alone or TMZ alone (Fig. 5A). To further demonstrate that the mechanism of miR-155 knockdown affects TMZ chemosensitivity, ROS production and cells apoptosis were measured. The results showed that TMZ promoted the production of ROS, and knockdown of miR-155 increased the ability of TMZ to promote ROS production (Fig. 5B upper pannel). N-acetylcysteine(NAC) is a ROS inhibitor that can inhibit intracellular ROS production. NAC treatment significantly blocked the effects on ROS production from miR-155 inhibitor or TMZ (Fig. 5B low panel, left). At the same time, interfering MAPK13 or MAPK14 can inhibit the production of ROS (Fig. 5B low panel, right).

Additionally, Hoechst 33258 (Fig. 5C) and Annexin V assay (Fig. 5D) were used to detect cell apoptosis. The results indicated that knockdown of miR-155 increased the apoptosis of U87 cells that was induced by TMZ. We also detected the effect of MAPK13 and MAPK14 siRNA on apoptosis, MAPK13 and MAPK14 siRNA can inhibit cell apoptosis by Hoechst 22358 (data not shown). And the

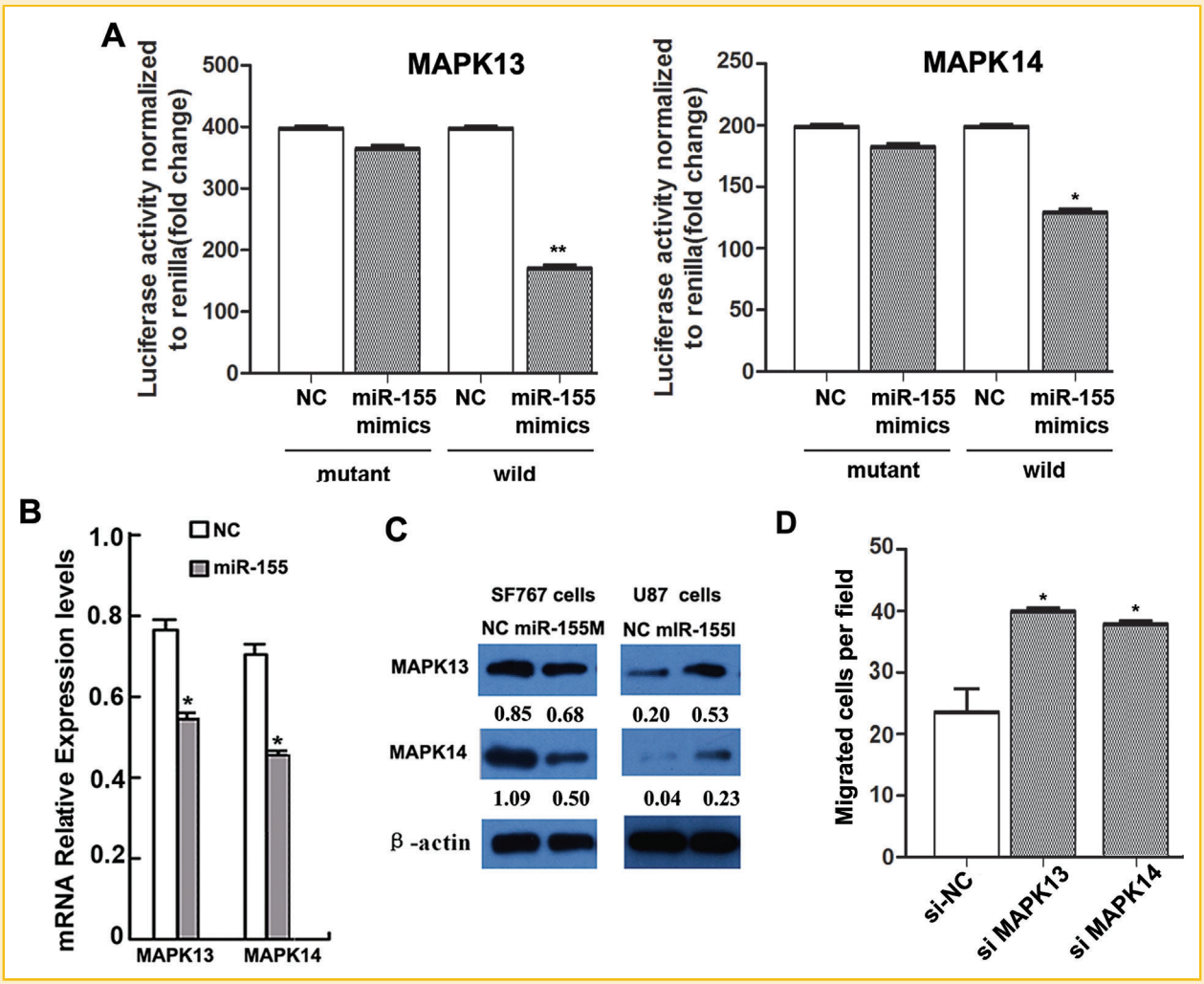

Fig. 3. miR-155 promotes cell invasion by targeting MAPK13 and MAPK14 in glioma cells. A: Luciferase activity assay for the binding of miR-155 to MAPK13 or MAPK14. *P-value <0.05 versus NC; ** P-value <0.01 versus NC. B: Transfection of miR-155 decreased the mRNA expression of MAPK13 or MAPK14 by real-time PCR. *P-value <0.05 versus NC. C: The western blot shows that transfection of miR-155 decreased the protein expression of MAPK13 or MAPK14 in SF767 cells. Transfection of the miR-155 inhibitor decreased the protein expression of MAPK13 or MAPK14 in U87 cells. D: The Matrigel matrix invasion assay was used to detect the effect of MAPK13 siRNA or MAPK14 siRNA on glioma cells. MAPK13 or MAPK14 siRNA promoted the invasion of SF767 cells. The histogram represents the mean of invasive cells which was determined by counting cells in four microscopic fields per well. The experiments were repeated three times. *P-value <0.05 vs. siNC.

effect that knockdown of miR-155 decreased the cells proliferation and increased the ROS production and apoptosis which induced by TMZ due to inhibition of MAPK13 and MAPK14 expression (Fig. 5E). However, the combined treatment of miR-155 knockdown and TMZ did not show synergistic inhibition on the secretion of MMP2 and MMP9 when compared with the knockdown of miR-155 alone or TMZ alone in U87 cells (Fig. 5F).

DISCUSSION

Glioma is the most common malignant primary tumor of the brain and usually has a poor prognosis [Zhang et al., 2008]. Even with improved therapy regimens including the drug TMZ, the survival rate is not ideal. miRNAs are a kind of gene expression regulators, which can directly regulate the expression of target genes to play an important roles in cells proliferation, apoptosis and survival [Tang et al., 2012, 2013]. For example, miR-211 can influence the cell chemosensitivity and radiosensitivity by MMP9 [Asuthkar et al., 2012]. The expression of miR-155 is overexpressed in many tumors, such as lung cancer, glioblastoma and leukmias [Poltronieri et al., 2013]. Here, we provide evidence that miR-155 is highly expressed in glioma tissues. Overexpression of miR-155 promoted cell proliferation, invasion, and migration in SF767 cells, which normally have low expression of miR-155. Anti-miR-155 treatments inhibited cell proliferation, invasion, and migration in U87 cells, which normally have higher expression of miR-155. Our research further confirmed that knockdown of miR-155 is a potentially useful therapy target for

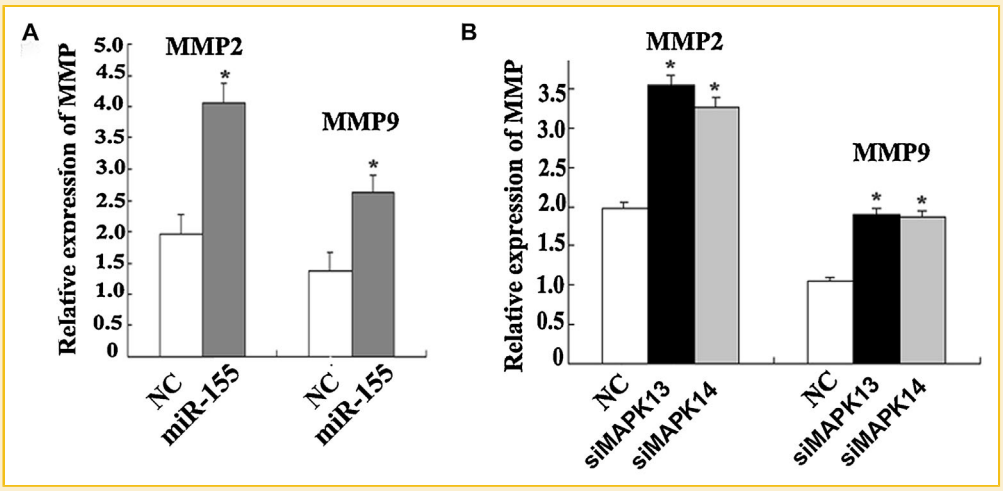

Fig. 4. Effect of miR-155, MAPK13 siRNA or MAPK14 siRNA on the secretion of MMP2 and MMP9. A: Supernatants were collected after SF767 cells were treated with miR-155 for 24 h. The MMP2 and MMP9 secretion levels in SF767 cells were analyzed using an ELISA assay kit. The relative secretion expression compared with NC is shown. **P*-value <0.05 versus NC. B: Supernatants were collected after SF767 cells were treated with MAPK13 siRNA or MAPK14 siRNA for 24 h. MMP2 and MMP9 secretion levels in SF767 cells were analyzed using an ELISA assay kit, and the relative secretion expression compared with the siRNA control is shown. **P*-value <0.05 versus NC.

glioma [Poltronieri et al., 2013]. However, the mechanism of miR-155 in anti-cancer therapy is still unknown.

In this study, we predicted and confirmed that the p38 isoforms MAPK13 and MAPK14 are targets of miR-155. p38 is a component of the MAPK signaling pathway and is a serine/threonine protein kinase. The p38-MAPK pathway plays an important role in the cellular response to various types of stress, including cancer [Kumphune et al., 2013]. Chlorpyrifos (CPF), a pesticide that activates the p38-MAPK signaling pathway, mediates apoptosis by generating ROS [Ki et al., 2013]. MAPK13 and MAPK14 are the p38 isoforms. MAPK13 encodes p38δ, and e pigenetic silencing of MAPK13 contributes to melanoma progression. MAPK13 re-expression restored the tumor suppressive functions in melanoma cells [Gao et al., 2013]. Upon silencing ATP5A1, the expression of MAPK13 was upregulated by oxidative stress due to impaired ATP synthesis[Anitha et al., 2013]. MAPK14 encodes p38α/MAPK, which can inhibit liver fibrogenesis and consequently hepatocarcino-genesis by reducing the accumulation of reactive oxygen species [Sakurai et al., 2013]. The synthetic flavonoid WYC02–9 activated MAPK14 pathway to block the cells growth through the ROS in colorectal carcinoma [Chen et al., 2013]. Our data showed that the expression of MAPK13 and MAPK14, as target genes of miR-155, is downregulated with miR-155 treatment in SF767 cells. Furthermore, the expression of MAPK13 and MAPK14 was upregulated under the knockdown of miR-155 in U87 cells.

Under pathological condition, matrix metalloproteinases (MMPs) is activated, especially gelatimases MMP2 and MMP9, and mainly involved in cell migration, invasion and angiogenesis [Tarassishin and Lee, 2013]. Our studies indicated that overexpression of miR-155 promoted the secretion of MMP2 and MMP9 in the supernatant of SF767 cells. Additionally, interfering with MAPK13 or MAPK14 also increased the secretion of MMP2 and MMP9 in the supernatant of SF767 cells, suggesting that miR-155 can increase the secretory expression of MMP2 and MMP9. Thus, miR-155 may be involved in the invasive proliferation of glioma cells by targeting and inhibiting MAPK13 or MAPK14.

Malignant gliomas are treated with a combination of surgery, radiation, and chemotherapy drugs such as temozolomide (TMZ), but these therapies ultimately fail due to tumor recurrence [Wan et al., 2013]. MicroRNAs are aberrantly expressed in many cancers and can exert tumor-suppressive or oncogenic functions. Oncomirs usually promote cells proliferation and invasion during chemotherapy, therefore, combining with chemotherapy drugs and oncomirs silence are a valuable approach for cancers [Meng et al., 2012]. In this study, we aimed to identify the combined effects of knockdown of miR-155 and TMZ on the invasive pathogenesis of glioma cells. Knockdown of miR-155 increased the inhibitory effect of TMZ on U87 cells proliferation and increased the TMZ-induced ROS production. There is an effective strategy for destroy cancer stem cells by regulating ROS generation [Diehn et al., 2009]; however, p38 MAPK signaling can mediate apoptosis by generating ROS [Ki et al., 2013]. Our findings suggested that knockdown of miR-155 enhanced the anticancer effect of TMZ on gliomas through MAPK13 and MAPK14-mediated ROS accumulation. However, knockdown of miR-155 did not increase the secretion of MMP2 and MMP9 that was induced by TMZ. It is possible that there is another mechanism involved in the effect of the knockdown of miR-155 on TMZ induced- secretion of MMP2 and MMP9. The aim of our future studies will be to examine whether the knockdown of miR-155 can affect TMZ induced-activation of MMP2 and MMP9.

CONCLUSIONS

The increased expression of miR-155 is implicated in glioma carcinogenesis. Knockdown of miR-155 inhibits the invasive

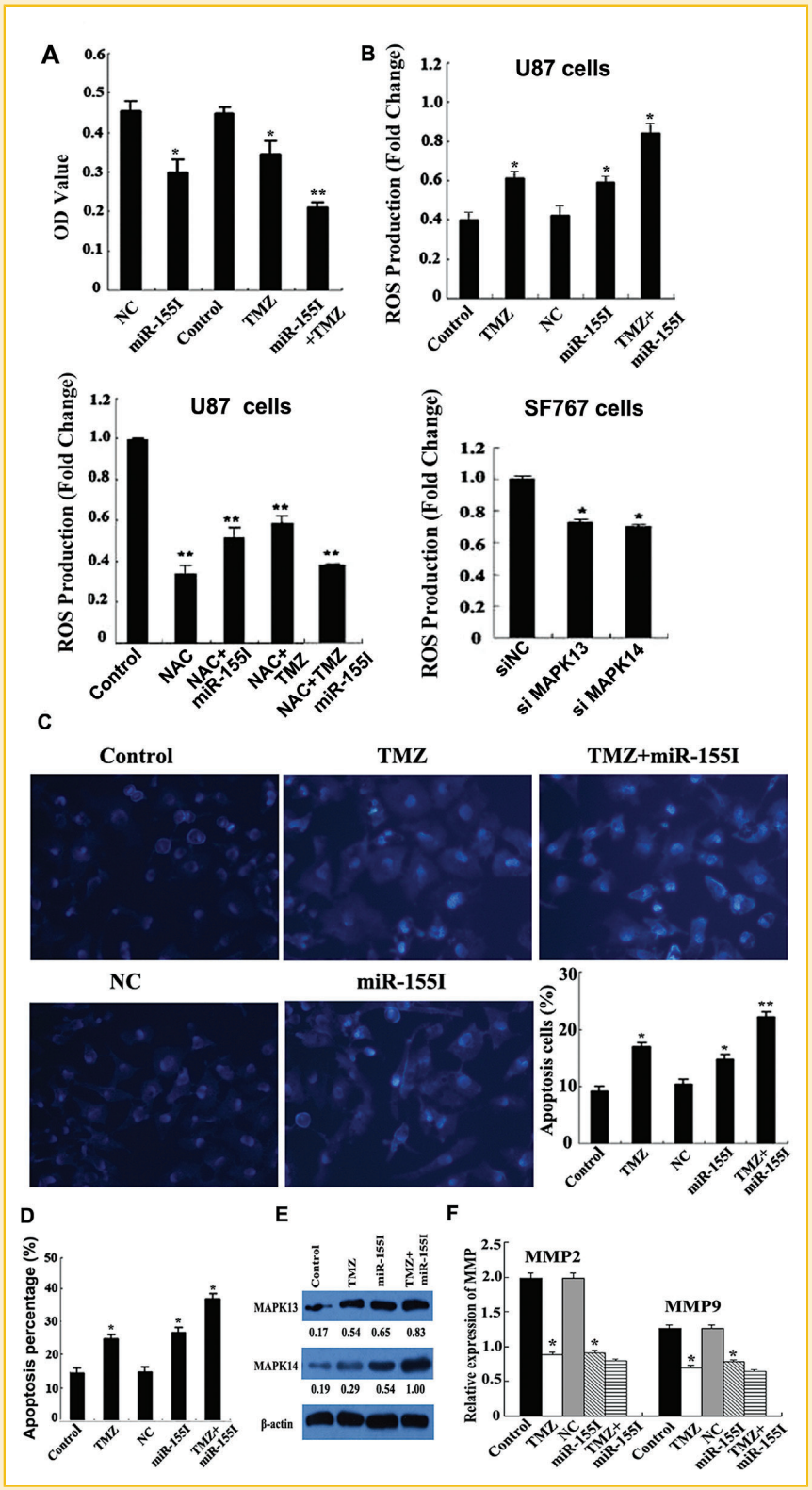

Fig. 5. Knockdown of miR-155 sensitizes cells to chemotherapy in gliomas through ROS-induced apoptosis. A: The MTT assay indicated that the combined knockdown of miR-155 and TMZ resulted in a distinct decrease in U87 cell proliferation compared with miR-155 knockdown alone or TMZ alone. **P*-value <0.05 vs. NC or control; ***P*-value <0.05 vs. TMZ or miR-155I. TMZ: 100 μM, miR-155I:20μM. B: Upper panel: The DCHF-DA assay indicated that the combined miR-155I and TMZ increased the induction of ROS production in U87 cells compared with miR-155 knockdown alone or TMZ alone. **P*-value <0.05 versus control or NC; ***P*-value <0.05 versus TMZ or miR-155I. TMZ: 100 μM, miR-155I:20μM. Lower panel (Left): The ROS inhibitor NAC blocked the effect of miR-155I or/and TMZ on ROS production in U87 cells. ***P*-value <0.01 versus control. Lower panel (Right): The knockdown of MAPK13 or MAPK14 inhibited ROS production in SF767 cells. **P*-value <0.05 versus siNC. C: The Hoechst 33258 staining indicated that the knockdown of miR-155 increased the cell apoptosis induced by TMZ in U87 cells compared with miR-155 knockdown alone or TMZ alone. **P*-value <0.05 versus control or NC; ***P*-value <0.05 versus TMZ or miR-155I. TMZ: 100 μM, miR-155I:20μM. D: Annexin V assay indicated that the knockdown of miR-155 increased the cell apoptosis induced by TMZ in U87 cells compared with miR-155 knockdown alone or TMZ alone. **P*-value <0.05 versus control or NC; ***P*-value <0.05 versus TMZ or miR-155I. TMZ: 100 μM, miR-155I:20μM. E: The western blot assay indicated that the combined knockdown of miR-155 and TMZ increased the expression of MAPK13 or MAPK14 in U87 cells compared with miR-155 knockdown alone or TMZ alone. β-actin was used as an internal reference for loading. TMZ: 100 μM, miR-155I:20μM. F: The ELISA assay indicated that the combined treatment of miR-155 knockdown and TMZ did not synergistically affect the secretion of MMP2 and MMP9 compared with miR-155 knockdown alone or TMZ alone. **P*-value <0.05 versus control or NC TMZ: 100 μM, miR-155I:20μM.

proliferation of glioma cells by targeting the p38 isoforms. The knockdown of miR-155 enhanced the anticancer effect of temozolomide on glioma cells through the induction of MAPK13 and MAPK14-mediated oxidative stress and apoptosis. Thus, miR-155 may be a potential target for glioma therapy.

REFERENCES

Anitha A, Nakamura K, Thanseem I, Matsuzaki H, Miyachi T, Tsujii M, Iwata Y, Suzuki K, Sugiyama T, Mori N. 2013. Downregulation of the expression of mitochondrial electron transport complex genes in autism brains. Brain Pathol 23:294–302.

Asuthkar S, Velpula KK, Chetty C, Gorantla B, Rao JS. 2012. Epigenetic regulation of miRNA-211 by MMP-9 governs glioma cell apoptosis, chemosensitivity and radiosensitivity. Oncotarget 3:1439–1454.

Bartel DP. 2004. MicroRNAs: Genomics, biogenesis, mechanism, and function. Cell 116:281–297.

Chen YJ, Chen HP, Cheng YJ, Lin YH, Liu KW, Chen YJ, Hou MF, Wu YC, Lee YC, Yuan SS. 2013. The synthetic flavonoid WYC02–9 in hibits colorectal cancer cell growth through ROS-mediated activation of MAPK14 pathway. Life Sci 92:1081–1092.

Diehn M, Cho RW, Lobo NA, Kalisky T, Dorie MJ, Kulp AN, Qian D, Lam JS, Ailles LE, Wong M, Joshua B, Kaplan MJ, Wapnir I, Dirbas FM, Somlo G, Garberoglio C, Paz B, Shen J, Lau SK, Quake SR, Brown JM, Weissman IL, Clarke MF. 2009. Association of reactive oxygen species levels and radioresistance in cancer stem cells. Nature 458:780–783.

D′Urso PI, D′Urso OF, Storelli C, Mallardo M, Gianfreda CD, Montinaro A, Cimmino A, Pietro C, Marsigliante S. 2012. MiR-155 is up-regulated in primary and secondary glioblastoma and promotes tumour growth by inhibiting GABA receptors. Int J Oncol 41:228–234.

Eis PS, Tam W, Sun L, Chadburn A, Li Z, Gomez MF, Lund E, Dahlberg JE. 2005. Accumulation of miR-155 and BIC RNA in human B cell lymphomas. Proc Natl Acad Sci USA 102:3627–3632.

Gao L, Smit MA, van den Oord JJ, Goeman JJ, Verdegaal EM, van der Burg SH, Stas M, Beck S, Gruis NA, Tensen CP, Willemze R, Peeper DS, van Doorn R. 2013. Genome-wide promoter methylation analysis identifies epigenetic silencing of MAPK13 in primary cutaneous melanoma. Pigment Cell Melanoma Res 26:542–554.

Iorio MV, Ferracin M, Liu CG, Veronese A, Spizzo R, Sabbioni S, Magri E, Pedriali M, Fabbri M, Campiglio M, Ménard S, Palazzo JP, Rosenberg A, Musiani P, Volinia S, Nenci I, Calin GA, Querzoli P, Negrini M, Croce CM. 2005. MicroRNA gene expression deregulation in human breast cancer. Cancer Res 65:7065–7070.

Ki YW, Park JH, Lee JE, Shin IC, Koh HC. 2013. JNK and p38 MAPK regulate oxidative stress and the inflammatoryresponse in chlorpyrifos-induced apoptosis. Toxicol Lett 218:235–245.

Kumphune S, Chattipakorn S, Chattipakorn N. 2013. Roles of p38-MAPK in insulin resistant heart: Evidence from bench for future bedside application. Curr Pharm Des 19:5742–5754.

Lee HW, Lee EH, Ha SY, Lee CH, Chang HK, Chang S, Kwon KY, Hwang IS, Roh MS, Seo JW. 2012. Altered expression of microRNA miR-21, miR-155, and let-7a and their roles in pulmonary neuroendocrine tumors. Pathol Int 62:583–591.

Li M, Liu J, Zhang C. 2011. Evolutionary history of the vertebrate mitogen activated proteinkinases family. PLoS One 6:e26999.

Liu R, Liao J, Yang M, Shi Y, Peng Y, Wang Y, Pan E, Guo W, Pu Y, Yin L. 2012. Circulating miR-155 expression in plasma: a potential biomarker for early diagnosis of esophageal cancer in humans. J Toxicol Environ Health A 75:1154–1162.

Mattiske S, Suetani RJ, Neilsen PM, Callen DF. 2012. The oncogenic role of miR-155 in breast cancer. Cancer Epidemiol Biomarkers Prev 21:1236–1243.

Meng W, Jiang L, Lu L, Hu H, Yu H, Ding D, Xiao K, Zheng W, Guo H, Ma W. 2012. Anti-miR-155 oligonucleotide enhances chemosensitivity of U251 cell to taxol by inducing apoptosis. Cell Biol Int 36:653–659.

Ohgaki H, Kleihues P. 2005. Epidemiology and etiology of gliomas. Acta Neuropathol 109:93–108.

Paillas S, Causse A, Marzi L, de Medina P, Poirot M, Denis V, Vezzio-Vie N, Espert L, Arzouk H, Coquelle A, Martineau P, Del Rio M, Pattingre S, Gongora C. 2012. MAPK14/p38α confers irinotecan resistance to TP53-defective cells by inducing survival autophagy. Autophagy 8:1098–1112.

Poltronieri P, D′Urso PI, Mezzolla V, D′Urso OF. 2013. Potential of anti-cancer therapy based on anti-miR-155 oligonucleotides in glioma and brain tumours. Chem Biol Drug Des 81:79–84.

Sakurai T, Kudo M, Umemura A, He G, Elsharkawy AM, Seki E, Karin M. 2013. P38α inhibits liver fibrogenesis and consequent hepatocarcinogenesis by curtailing accumulation of reactive oxygen species. Cancer Res 73:215–224.

Sandhu SK, Volinia S, Costinean S, Galasso M, Neinast R, Santhanam R, Parthun MR, Perrotti D, Marcucci G, Garzon R, Croce CM. 2012. MiR-155 targets histone deacetylase 4 (HDAC4) and impairs transcriptional activity of B-cell lymphoma 6 (BCL6) in the Eμ-miR-155 transgenic mouse model. Proc Natl Acad Sci USA 109:20047–20052.

Slattery ML, John E, Torres-Mejia G, Stern M, Lundgreen A, Hines L, Giuliano A, Baumgartner K, Herrick J, Wolff RK. 2013. Matrix metalloproteinase genes are associated with breast cancer risk and survival: The breast cancer health disparities study. PLoS ONE 8:e63165.

Tan FL, Ooi A, Huang D, Wong JC, Qian CN, Chao C, Ooi L, Tan YM, Chung A, Cheow PC, Zhang Z, Petillo D, Yang XJ, Teh BT. 2010. P38delta/MAPK13 as a diagnostic marker for cholangiocarcinoma and its involvement in cell motility and invasion. Int J Cancer 126:2353–2361.

Tang H, Wang Z, Liu X, Liu Q, Xu G, Li G, Wu M. 2012. LRRC4 inhibits glioma cell growth and invasion through a miR-185-dependent pathway. Curr Cancer Drug Targets 12:1032–1042.

Tang H, Bian Y, Tu C, Wang Z, Yu Z, Liu Q, Xu G, Wu M, Li G. 2013. The miR-183/96/182 Cluster Regulates Oxidative Apoptosis and Sensitizes Cells to Chemotherapy in Gliomas. Curr Cancer Drug Targets 13:221–231.

Tarassishin L, Lee SC. 2013. Interferon regulatory factor 3 alters glioma inflammatory and invasive properties. J Neurooncol 113:185–194.

Tay Y, Zhang J, Thomson AM, Lim B, Rigoutsos I. 2008. MicroRNAs to Nanog, Oct4 and Sox2 coding regions modulate embryonic stem cell differentiation. Nature 455:1124–1128.

Volinia S, Calin GA, Liu CG, Ambs S, Cimmino A, Petrocca F, Visone R, Iorio M, Roldo C, Ferracin M, Prueitt RL, Yanaihara N, Lanza G, Scarpa A, Vecchione A, Negrini M, Harris CC, Croce CM. 2006. A microRNA expression signature of human solid tumors defines cancer gene targets. Proc Natl Acad Sci USA 103:2257–2261.

Wan Y, Sun G, Zhang S, Wang Z, Shi L. 2013. MicroRNA-125b inhibitor sensitizes human primary glioblastoma cells to chemotherapeutic drug temozolomide on invasion. In Vitro Cell Dev Biol Anim 49:599–607.

Yang M, Shen H, Qiu C, Ni Y, Wang L, Dong W, Liao Y, Du J. 2013. High expression of miR-21 and miR-155 predicts recurrence and unfavourable survival in non-small cell lung cancer. Eur J Cancer 49:604–615.

Zhang Z, Li D, Wu M, Xiang B, Wang L, Zhou M, Chen P, Li X, Shen S, Li G. 2008. Promoter hypermethylation-mediated inactivation of LRRC4 in gliomas. BMC Mol Biol 9:99DOI: 10.1186/1471–2199-9–99.